Model Predictive Control using Linearized Radial Basis Function Neural Models for Water Distribution Networks

Balla, Krisztian Mark; Nørgaard Jensen, Tom; Bendtsen, Jan Dimon; Kallesøe, Carsten

Published in:
2019 IEEE Conference on Control Technology and Applications (CCTA)

DOI (link to publication from Publisher):
10.1109/CCTA.2019.8920627

Publication date:
2019

Document Version
Publisher's PDF, also known as Version of record

2019 IEEE Conference on Control Technology and Applications (CCTA)
Hong Kong, China, August 19-21, 2019

Model Predictive Control using linearized Radial Basis Function Neural Models for Water Distribution Networks

Krisztian Mark Balla[1,2], Tom Nørgaard Jensen[3], Jan Dimon Bendtsen[1] and Carsten Skovmose Kallesøe[1,2]

***Abstract*— It is often the case that the main operation cost of Water Distribution Networks (WDN) is due to pump actuation. Although advanced control schemes are widely available, most water utilities still use on/off control. In this study, water networks with multiple flow inlets, storage tanks and several consumers are considered. Under mild assumptions on the consumption and hydraulic resistance of pipes, a reduced model is proposed with the aim of building its mathematical structure into a data-driven control design. For identification purposes we use Radial Basis Function Neural Networks (RBFNN). We show that linearization of the identified RBFNN model in the two peak points of the daily flow demand results in a control model with good prediction accuracy. Subsequently, this time-varying model is utilized in a standard economic Model Predictive Control (MPC) scheme, considering pump flows as inputs. A numerical case study on an EPANET[4] model and experimental results on a test setup demonstrate the proposed method.**

I. INTRODUCTION

Water Distribution Networks (WDN) are among the most vital infrastructures of modern societies. They consist of a large number of hydraulic elements, such as elevated reservoirs, pressurized pipelines, pumping stations and valves. Although elevated reservoirs are often an integrated part of these networks, water utilities rarely use their storage capability for optimization. This paper deals with optimization of reservoir filling via flow set-point control for multiple pumping stations. Optimality here is measured as the minimum economic cost for pump operation.

Model Predictive Control (MPC) is a well-suited approach for cost-efficient WDN management when operational constraints are considered. In particular, MPC has been investigated and successfully implemented in many research papers. In [2] and [3], optimal flow-set points for pumps are computed by solving a finite-horizon optimization problem including economic costs with operational constraints, while considering only the pipe flows as the system variables. In [4] and [5], distributed and decentralized MPC is considered, respectively. The paper [6] considers the non-linearity of WDNs using a constraint satisfaction formulation. MPC has shown good results in large-scale water applications, given that a model of the WDN dynamics was available. However, such models lead to high costs of maintenance. Therefore, detailed models are typically economically out of reach at small water utilities.

[1]Aalborg University, Fredrik Bajers vej 7c, DK-9220 Aalborg, Denmark, Email: {kmb,dimon,csk}@es.aau.dk
[2]Grundfos A/S, Poul Due Jensens vej 7, DK-8850 Bjerringbro, Denmark, Email: {kballa,ckallesoe}@grundfos.com
[3]Independent researcher, Aalborg, Denmark
[4]EPANET is a standard modelling tool used at many water utilities [1]

The main contribution of this paper comprises an extension of the work in [7] and [8], where reduced network models have been proposed for networks without elevated reservoirs. Additionally, [9] focuses on Plug&Play MPC where a heuristic model of a WDN with one pumping station and one elevated reservoir is considered. In particular, here we consider networks with multiple inlets and multiple storage tanks and seek to establish a control-oriented model, relying only on the reduced model structure and on measurement data. The outcome is an MPC scheme which utilizes such a model.

The paper is organized as follows. In **Section II**, the preliminary study of reduced network modelling, network partitioning and the inclusion of reservoir dynamics is presented. In **Section III**, the developed model is used for system identification by using Neural Networks (NN). Moreover, an internal MPC model is obtained by linearizing the NN in different Operating Points (OP). In **Section IV**, the linearized models are used in a MPC scheme. **Section V** presents numerical and experimental results regarding modelling and control. The paper ends with some remarks and conclusions.

a) *Nomenclature:* Let $\langle x, y\rangle$ denote the scalar product between two vectors $x, y \in \mathbb{R}^n$. We say a map $f : \mathbb{R}^n \to \mathbb{R}^n$ is (strictly) monotonic increasing if $\langle x-y, f(x)-f(y)\rangle \geq (>)0\ \forall x, y \in \mathbb{R}^n$ such that $x \neq y$. With $M(n, m; X)$ we denote the set of n-by-m matrices whose entries belong to the set X. By $\mathbb{1}_n$ we denote the n-dimensional vector consisting of ones. $||\cdot||$ is the Euclidean norm.

II. NETWORK MODEL

A. Preliminaries

WDNs can be described by a directed and connected graph $\mathcal{G} = \{\mathcal{V}, \mathcal{E}\}$. The elements of the set $\mathcal{V} = \{v_1, ..., v_n\}$ are denoted vertices and represent pipe connections with possible end-user water consumption or storage elements. The elements of the set $\mathcal{E} = \{e_1, ..., e_m\}$ are denoted edges and represent pipes. The demand at vertex i is denoted d_i, and the pressure drop due to elevation by h_i. The pressure drop due to friction over edge j is denoted by f_j, and this pressure drop is a function of the flow q_j through the pipe j. To the graph $\mathcal{G}$, we associate the incidence matrix H

$$H_{i,j} = \begin{cases} -1\ , & \text{if the } j^{th} \text{ edge is entering } i^{th} \text{ vertex.} \\ 0\ , & \text{if the } j^{th} \text{ edge is not connected to the } i^{th} \text{ vertex.} \\ 1\ , & \text{if the } j^{th} \text{ edge is leaving } i^{th} \text{ vertex.} \end{cases}$$

We see that $H \in M(n, m; \{-1, 0, 1\})$, where m is the number of edges and n is the number of vertices.

The network must fulfill Kirchhoff's vertex law, which corresponds to conservation of mass in each vertex:

$$Hq = d, \tag{1}$$

where $q \in \mathbb{R}^m$ is the vector of flows and $d \in \mathbb{R}^n$ is the vector of nodal demands. Reservoir flows with $d_i > 0$ when flow is into vertex i.

Let p_i denote the absolute pressure at vertex i. Then, the infinitesimal pressure increase in elevated reservoirs is:

$$\dot{p}_i = -\frac{\rho g}{A_i} d_i, \tag{2}$$

where A_i is the constant cross section of the reservoir, ρ is water density and g is the gravitational constant.

Let p be the vector of absolute pressures at vertices and Δp the vector of differential pressures across the connecting edges. Then, the "Ohm law" for water networks gives

$$\Delta p = H^T p = f(q) - (H^T h), \tag{3}$$

where $p \in \mathbb{R}^n$, $f : \mathbb{R}^m \to \mathbb{R}^m$, $f(q) = (f_1(q_1), ..., f_m(q_m))$ with f_i strictly increasing. The last term in (3) is the pressure drop due to elevation differences at the pipe ends.

Assumption 1 *The hydraulic resistance $f_i : \mathbb{R} \to \mathbb{R}$ takes the form $f_i(q_i) = \rho_i |q| q$ with $\rho_i > 0$ a constant pipe parameter. This form is motivated by turbulent flow, which is typical in WDNs [10].*

B. Network partitioning

As an addition to the results in [8], we seek to derive a reduced network model which captures the dynamics of elevated reservoirs. To this end, we consider the partitioning of the network graph such that we let the set $\hat{\mathcal{V}} = \{\hat{v}_1, ..., \hat{v}_l\}$ with $l \geq 1$ represent vertices corresponding to elevated reservoirs. The set $\bar{\mathcal{V}} = \{\bar{v}_1, ..., \bar{v}_{n-l}\}$ represents the remaining vertices in the graph. Furthermore, $\mathcal{E} = \{\mathcal{E}_\mathcal{T}, \mathcal{E}_\mathcal{C}\}$ is a partitioning of edges such that the incidence matrix is

$$H = \begin{bmatrix} \bar{H}_\mathcal{T} & \bar{H}_\mathcal{C} \\ \hat{H}_\mathcal{T} & \hat{H}_\mathcal{C} \end{bmatrix}, \tag{4}$$

where $\bar{H}_\mathcal{T}$ is square and invertible, which is always possible since $\mathcal{G}$ is a connected graph [11]. With the chosen partitioning, we can rewrite (1) and (3) to the following

$$\bar{d} = \bar{H}_\mathcal{T} q_\mathcal{T} + \bar{H}_\mathcal{C} q_\mathcal{C}, \tag{5a}$$
$$\hat{d} = \hat{H}_\mathcal{T} q_\mathcal{T} + \hat{H}_\mathcal{C} q_\mathcal{C}, \tag{5b}$$
$$f_\mathcal{T}(q_\mathcal{T}) = \bar{H}_\mathcal{T}^T(\bar{p} + \bar{h}) + \hat{H}_\mathcal{T}^T(\hat{p} + \hat{h}), \tag{5c}$$
$$f_\mathcal{C}(q_\mathcal{C}) = \bar{H}_\mathcal{C}^T(\bar{p} + \bar{h}) + \hat{H}_\mathcal{C}^T(\hat{p} + \hat{h}), \tag{5d}$$

where $\hat{d}, \hat{p} \in \mathbb{R}^l$ represent the vector of tank flows and tank pressures, respectively. From (5a) we can derive an expression for the vector $q_\mathcal{T}$ of flows

$$q_\mathcal{T} = -\bar{H}_\mathcal{T}^{-1} \bar{H}_\mathcal{C} q_\mathcal{C} + \bar{H}_\mathcal{T}^{-1} \bar{d}. \tag{6}$$

Using (5c), (5d) and (6), the following is derived

$$f_\mathcal{C}(q_\mathcal{C}) - \bar{H}_\mathcal{C}^T \bar{H}_\mathcal{T}^{-T} f_\mathcal{T}(-\bar{H}_\mathcal{T}^{-1} \bar{H}_\mathcal{C} q_\mathcal{C} + \bar{H}_\mathcal{T}^{-1} \bar{d}) = (\hat{H}_\mathcal{C}^T - \bar{H}_\mathcal{C}^T \bar{H}_\mathcal{T}^{-T} \hat{H}_\mathcal{T}^T)(\hat{p} + \hat{h}). \tag{7}$$

Next, using (5c) and (6), we obtain the vector of pressures at vertices not associated to elevated reservoirs

$$\bar{p} = \bar{H}_\mathcal{T}^{-T} f_\mathcal{T}(-\bar{H}_\mathcal{T}^{-1} \bar{H}_\mathcal{C} q_\mathcal{C} + \bar{H}_\mathcal{T}^{-1} \bar{d}) - \bar{H}_\mathcal{T}^{-T} \hat{H}_\mathcal{T}^T(\hat{p} + \hat{h}) - \bar{h}. \tag{8}$$

In order to distinguish between inlet and non-inlet points, the vertices in set $\bar{\mathcal{V}}$ are further partitioned such that

$$\bar{p} = K \bar{p}_\mathcal{K} + D \bar{p}_\mathcal{D} \quad , \quad \bar{d} = K \bar{d}_\mathcal{K} + D \bar{d}_\mathcal{D}, \tag{9}$$

where $\bar{d}_\mathcal{K}, \bar{p}_\mathcal{K} \in \mathbb{R}^c$ are inlet flows and pressures. $\bar{d}_\mathcal{D}, \bar{p}_\mathcal{D} \in \mathbb{R}^{n-l-c}$ are non-inlet flows and pressures, respectively. Furthermore, $\bar{p}_\mathcal{K} = K^T \bar{p}$ and $\bar{p}_\mathcal{D} = D^T \bar{p}$. The distribution of flow demands is formulated in Assumption 2.

Assumption 2 *It is assumed that the distribution between the $n - l - c$ free nodal demands in $\bar{d}_\mathcal{D}(t)$ is fixed, that is $\bar{d}_\mathcal{D}(t) = v_\mathcal{D} \sigma(t)$, where $v_\mathcal{D} \in \mathbb{R}^{n-l-c}$ with $v_{\mathcal{D},i} \in (0; 1)$ is a vector with the property $\sum_{i=1}^{n-l-c} v_{\mathcal{D},i} = 1$ and $\sigma(t) < 0$ is the total consumption.*

C. Inclusion of elevated reservoirs

In contrast to the model in [8], elevated reservoirs add integrator-type dynamics to the pipe grid as shown in Fig. 1. In the following, we consider $l \geq 1$ number of tanks, where $\hat{p}$ pressure is measured. Additionally, $\bar{d}_\mathcal{K}$ and $\bar{p}_\mathcal{K}$ inlet flow and pressure are measured and certain critical pressure measurements $y_i \in \{\bar{p}_{\mathcal{D},1}, ..., \bar{p}_{\mathcal{D},n-l-c}\}$ are also available, where $n - l - c$ is the number of elements in $\bar{p}_\mathcal{D}$.

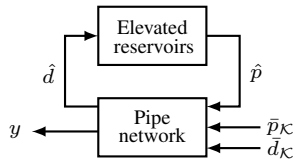

Fig. 1. Block structure of the extended network.

We express the tank flows by inserting the unknown $q_\mathcal{T}$ flows in (6) into Kirchhoff's law in (5b)

$$\hat{d} = (\hat{H}_\mathcal{C} - \hat{H}_\mathcal{T} \bar{H}_\mathcal{T}^{-1} \bar{H}_\mathcal{C}) q_\mathcal{C} + \hat{H}_\mathcal{T} \bar{H}_\mathcal{T}^{-1} \bar{d}. \tag{10}$$

Recalling the model of elevated reservoirs in (2) and inserting the corresponding vector of tank flows yields

$$\begin{aligned} \Lambda \dot{\hat{p}} &= -(\hat{H}_\mathcal{C} - \hat{H}_\mathcal{T} \bar{H}_\mathcal{T}^{-1} \bar{H}_\mathcal{C}) q_\mathcal{C} - \hat{H}_\mathcal{T} \bar{H}_\mathcal{T}^{-1} \bar{d} \\ &= -(\hat{H}_\mathcal{C} - \hat{H}_\mathcal{T} \bar{H}_\mathcal{T}^{-1} \bar{H}_\mathcal{C}) q_\mathcal{C} - \hat{H}_\mathcal{T} \bar{H}_\mathcal{T}^{-1} K \bar{d}_\mathcal{K} \\ &\quad - \hat{H}_\mathcal{T} \bar{H}_\mathcal{T}^{-1} D v_\mathcal{D} \sigma, \end{aligned} \tag{11}$$

where $\Lambda = \text{diag}(\frac{A_1}{\rho g}, ..., \frac{A_l}{\rho g})$. In the second line of (11), the inlet and non-inlet flows are partitioned and the non-inlet demand flows are expressed regarding Assumption 2.

Recalling the implicit expression in (7) for $q_\mathcal{C}$ flows, the partitioned inlet and non-inlet flows are substituted

$$f_\mathcal{C}(q_\mathcal{C}) - M_1(\hat{p} + \hat{h}) - M_2^T f_\mathcal{T}(M_2 q_\mathcal{C} + M_3 K \bar{d}_\mathcal{K} - M_3 D v_\mathcal{D} \sigma) = 0, \tag{12}$$

where $M_1 = (\hat{H}_\mathcal{C}^T - \bar{H}_\mathcal{C}^T \bar{H}_\mathcal{T}^{-T} \hat{H}_\mathcal{T}^T)$, $M_2 = \bar{H}_\mathcal{T}^{-1} \bar{H}_\mathcal{C}$ and $M_3 = \bar{H}_\mathcal{T}^{-1}$. By solving (12) for $q_\mathcal{C}$, the tank dynamics can be expressed in terms of flow inlets and flow consumption.

Although an analytical solution has not been found, the solution is known to be unique. It can be shown that the left hand side of (7) is a homeomorphism in $q_{\mathcal{C}}$, using similar arguments as in [7].

Using (9) and applying Assumption 2, the inlet and non-inlet pressures are given by (13) and (14), respectively

$$\begin{aligned}\bar{p}_{\mathcal{K}} &= K^T \bar{H}_{\mathcal{T}}^{-T} f_{\mathcal{T}}(-M_2 q_{\mathcal{C}} + M_3 K \bar{d}_{\mathcal{K}} - M_3 D v_{\mathcal{D}} \sigma) \\ &\quad - K^T \bar{H}_{\mathcal{T}}^{-T} \hat{H}_{\mathcal{T}}^{T} (\hat{p} + \hat{h}) - K^T \bar{h}, \qquad (13)\\ \bar{p}_{\mathcal{D}} &= D^T \bar{H}_{\mathcal{T}}^{-T} f_{\mathcal{T}}(-M_2 q_{\mathcal{C}} + M_3 K \bar{d}_{\mathcal{K}} - M_3 D v_{\mathcal{D}} \sigma) \\ &\quad - D^T \bar{H}_{\mathcal{T}}^{-T} \hat{H}_{\mathcal{T}}^{T} (\hat{p} + \hat{h}) - D^T \bar{h}. \qquad (14)\end{aligned}$$

It is shown in (11), (13) and (14), that the proposed model is subject to the algebraic constraint on $q_{\mathcal{C}}$ flows in (12).

III. System Identification

A. Radial Basis Function Approximation

The implicit expression in (12) sets constraints on $q_{\mathcal{C}}$ flows. The existence of a unique solution is known but not its structure. Thus, we write (12) explicitly

$$q_{\mathcal{C}} = \alpha(\hat{p}, \bar{d}_{\mathcal{K}}, \sigma), \qquad (15)$$

By inserting (15) into the tank model in (11) and into the pressure models in (13) and (14), we obtain the mapping

$$\bar{p}_j = \tilde{g}_j(\hat{p}, \bar{d}_{\mathcal{K}}, \sigma) + \tilde{a}_j \hat{p} + \tilde{b}_j \bar{h}, \quad j \in \{\mathcal{K}, \mathcal{D}\}, \qquad (16)$$

where the non-linear parts are governed by $\tilde{g}_j$ with unknown structure and the affine model parameters are collected in $\tilde{a}_j$ and $\tilde{b}_j \bar{h}$. Then the tank model yields

$$\dot{\hat{p}} = \tilde{g}_{\mathcal{W}}(\hat{p}, \bar{d}_{\mathcal{K}}, \sigma) + \tilde{a}_{\mathcal{W}} \hat{d}_{\mathcal{K}} + \tilde{b}_{\mathcal{W}} \sigma, \qquad (17)$$

where $\tilde{g}_{\mathcal{W}}$ captures the non-linearities and $\tilde{a}_W$, $\tilde{b}_{\mathcal{W}}$ the linear parameters. The mappings in (16) and (17) are abstractions of the reduced model based on the partitioning and the physical features of the grid. For $\tilde{g}_j$ and $\tilde{g}_{\mathcal{W}}$, we consider a "linear in parameters" structure, thus standard recursive methods can be used for system identification.

We use Radial Basis Function Neural Networks (RBFNNs) due to the simple structure and fast training process [12]. In addition, RBFNNs can approximate any multivariate continuous function on a compact domain to an arbitrary accuracy, given a sufficient number of neurons [13]. Therefore, given that the resistance terms $f_i(q_i)$ are continuous maps, approximation with RBFNNs is suitable to represent the non-linearities. The input data set we use is $u = \{\hat{p}, \bar{d}_{\mathcal{K}}, \sigma\}$. Then the the pressure approximation at inlet point $\mathcal{K}r$, with $r \in \{1, 2, ..., c\}$ is

$$\bar{p}_{\mathcal{K}r}(t_k) = \underbrace{\sum_{i=1}^{M} w_{\mathcal{K}r,i} \phi_i\big(u(t_k)\big)}_{\approx \tilde{g}_{\mathcal{K}r}(\hat{p}, \bar{d}_{\mathcal{K}}, \sigma)} + \sum_{j=1}^{l} \tilde{a}_{\mathcal{K}r,j} \hat{p}_j(t_k) + \tilde{b}_{\mathcal{K}r}, \qquad (18)$$

where M is the number of RBF neurons, w is the weight parameter and $\phi(u) = \exp\big(-\frac{||u-\mu||^2}{2\psi^2}\big)$ with μ center points and ψ spread parameters. The center of the basis functions are determined according to the distribution of the input data u, using k-means clustering algorithm, while the spread parameters ψ are fixed. The weights and the bias of the RBFNN are found with Least Squares(LS) method.

For the approximate of water pressure derivative in storage tank $\mathcal{W}$, we assume that samples at t_k $k \in \{1, ..., N\}$ are available for parameter identification and let $t_{k+1} - t_k = \delta t_k$. Then the gradient is given by forward Euler method

$$\frac{\hat{p}_{\mathcal{W}s}(t_{k+1}) - \hat{p}_{\mathcal{W}s}(t_k)}{\delta t_k} = \sum_{i=1}^{P} w_{\mathcal{W}s,i} \phi_i\big(u(t_k)\big) + \sum_{j=1}^{c} \tilde{a}_{\mathcal{W}s,j} \bar{d}_{\mathcal{K},j}(t_k) + \tilde{b}_{\mathcal{W}s} \sigma(t_k), \qquad (19)$$

where $s \in \{1, 2, ..., l\}$ and P is the number of RBF neurons. The model is identified by calculating parameters $w, \tilde{a}$ and $\tilde{b}$. $\bar{p}_{\mathcal{K}}$ and $\bar{p}_{\mathcal{D}}$ are identified with the same model structure.

B. Linear Time-varying model

We presented a reduced network model that predicts the pressure $\hat{p}$ in elevated reservoirs and describes the inlet and non-inlet pressures $\bar{p}$, given measurements of $\bar{d}_{\mathcal{K}}$ inlet flows, $\hat{p}$ tank pressures and based on an average daily consumption profile. σ is calculated using

$$\sigma(t_k) = \mathbb{1}_c^T \bar{d}_{\mathcal{K}}(t_k) + \mathbb{1}_l^T \hat{d}(t_k). \qquad (20)$$

We approximated $\tilde{g}_{\mathcal{K}}$, $\tilde{g}_{\mathcal{D}}$ and $\tilde{g}_{\mathcal{W}}$ with RBFNNs to model the non-linear system dynamics. In this paper, we refine the model such that it is suitable for standard MPC. Using the NN model for MPC imposes a model constraint that is likely to be non-convex and thus hard to solve with standard methods. Therefore, we attempt to find linear approximations of the NN model in different Operating Points (OP). For that reason, we use the Taylor series expansion of (18) and (19) and formulate a switching State Space model, where θ is the scheduling variable. The dynamics are given by

$$\Delta\hat{p}_{\mathcal{W}}(t_{k+1}) = \begin{bmatrix} A(\theta) & B_u(\theta) & B_d(\theta) \end{bmatrix} \begin{bmatrix} \Delta\hat{p}_{\mathcal{W}}(t_k) \\ \Delta\bar{d}_{\mathcal{K}}(t_k) \\ \Delta\sigma(t_k) \end{bmatrix}, \qquad (21a)$$

and the expression for the inlet pressures is

$$\Delta\bar{p}_{\mathcal{K}}(t_k) = \begin{bmatrix} C(\theta) & D_u(\theta) & D_d(\theta) \end{bmatrix} \begin{bmatrix} \Delta\hat{p}_{\mathcal{W}}(t_k) \\ \Delta\bar{d}_{\mathcal{K}}(t_k) \\ \Delta\sigma(t_k) \end{bmatrix}, \qquad (21b)$$

where A, B_u, B_d, C, D_u and D_d are constant for each value of θ. Variables denoted with Δ are small signal deviations from the current OP.

Although the daily demand differs between workdays and weekends, in the following we only consider the average value of the total demand on workdays and assume that $\sigma(t_k) = \sigma(t_{k+T})$, as depicted in Fig. 2.

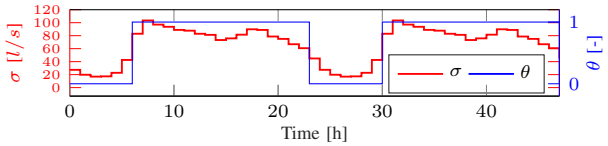

Fig. 2. Switching rule according to the total demand σ.

As shown in Fig. 2., parameter θ shifts with $T = 1$ day periodicity according to the lowest and highest daily consumption in the WDN. Correspondingly, the NN model is linearized at the two peak values of σ, therefore the shifting rule for all system matrices is

$$A(\theta) = \theta A^{max} + (1-\theta)A^{min}, \quad \theta \in \{0,1\}, \tag{22}$$

where A^{max} and A^{min} describe the models linearized in the two peak flow points, respectively. In the following, we refer to the switching model as Linear Time Varying (LTV).

IV. Predictive Control

We introduce a standard MPC scheme [14], that minimizes the cost of operating pumping stations. The control shifts the power consumption in time, such that tank capacity is used to minimize the operating costs subject to varying energy prices. The cost sequence $\mathcal{C}(t_k)$ is known in advance. We further assume such operating conditions that the efficiency of pumping stations are constant and identical [15].

The goal is to minimize the operating cost over a day by controlling $\bar{d}_{\mathcal{K}}$ inlet-flows. That is, we want to solve the convex optimization problem

$$\min_{\bar{d}_{\mathcal{K}}} \frac{1}{\eta} \sum_{i=0}^{H_p-1} \mathcal{C}(t_{k+i}|k)\bar{d}_{\mathcal{K}}^{T}(t_{k+i}|k)\bar{p}_{\mathcal{K}}(t_{k+i}|k) + \left(\hat{p}_{\mathcal{W}}(t_{0+H_p}) - \hat{p}_{\mathcal{W}}(t_0)\right)^2 \tag{23}$$

where η is the efficiency of all pumping stations and $H_p = 24$ hours is the prediction horizon. The term in the second line is introduced because the system is periodic and therefore the initial and final water pressure in the storage tanks should be equal over H_p. Furthermore, this optimization problem uses the internal model dynamics in (21). The operational and physical constraints are shown in (24).

$$0 < \bar{d}_{\mathcal{K}}^{min} \leq \bar{d}_{\mathcal{K}}(t_k) \leq \bar{d}_{\mathcal{K}}^{max}, \forall\, t_k \tag{24a}$$

$$0 < \hat{p}_{\mathcal{W}}^{min} \leq \hat{p}_{\mathcal{W}}(t_k) \leq \hat{p}_{\mathcal{W}}^{max}, \forall\, t_k \tag{24b}$$

$$0 < y^{min} \leq y(t_k) \leq y^{max}, \forall\, t_k, \tag{24c}$$

where (24a) describes the physical limitations on inlet flows. Furthermore, (24b) sets constraints on the minimum and maximum admissible storage volume in elevated reservoirs. Equation (24c) describes the constraints on the minimum and maximum pressure in the critical points of the network.

In standard MPC, the network dynamics are used to make predictions over H_p. In each initial time step t_k, the controller determines the OP which corresponds to the current peak or low consumption rates. The OP is kept constant over the predictions, meaning that we do not shift the model dynamics while we are in the current prediction horizon.

V. Results

Both numerical and experimental results demonstrate the proposed method in system identification and in MPC. In the EPANET environment [1], tank and inlet pressures are expressed in terms of length, e.g. water levels and pressure heads, respectively.

A. System identification

We show numerical results for comparing the performance of the Neural Network, LTV and high-fidelity EPANET models. For simulation, we use the EPANET model of the northern half of city Randers, located in Denmark. The network is illustrated in Fig. 3.

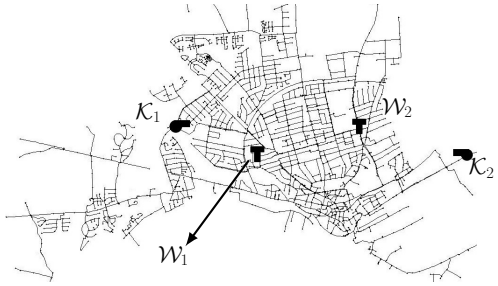

Fig. 3. EPANET model used for system identification and control.

This particular network consists of 3169 vertices and 3431 edges (n = 3169 and m = 3431). There are two inlet points $\mathcal{K}1$ and $\mathcal{K}2$, thus $\bar{d}_{\mathcal{K}} \in \mathbb{R}^2$ ($\bar{p}_{\mathcal{K}} \in \mathbb{R}^2$). Furthermore, there are two elevated reservoirs $\mathcal{W}1$ and $\mathcal{W}2$, thus $\hat{p}_{\mathcal{W}} \in \mathbb{R}^2$. Note that in this network critical points y have not been chosen. Fig. 4. shows the validation for the identified tank model.

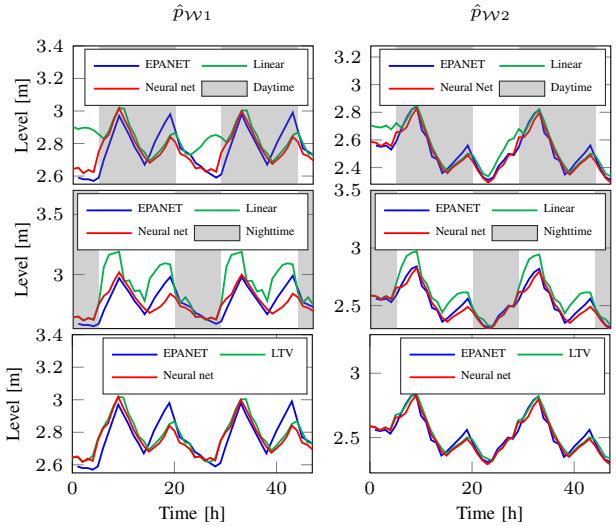

Fig. 4. Water level validation.

The first row shows the results using the RBFNN model linearized in σ^{max}, while the second row illustrates the results using the model linearized in σ^{min}. The last row shows the LTV model where we switch between the two local linear models. Fig. 5. shows validation results for the model describing the inlet pressures. Here we only show the results when we switch between the two OPs.

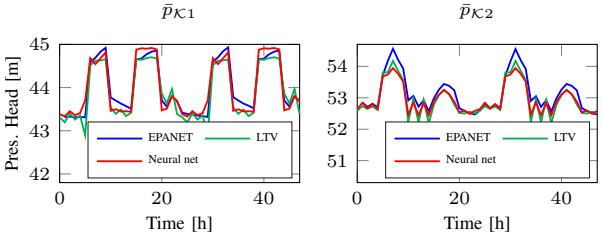

Fig. 5. Inlet pressure validation.

As shown in Fig 4., the local linear models describe the process accurately in the proximity of the OPs. We indicate this by distinguishing between days and nights, as the two average dominating flow consumption can be divided into these two periods. Furthermore, the model deviation is also expected since we know that the linearized NN cannot describe the non-linear process given that we assume large variations in the daily total flow consumption.

The identification and validation results show that switching between two OPs, corresponding to the two peak points of σ, results in good model accuracy. Note that the accuracy of the linear model dynamics depends on the accuracy of the NN model. Therefore, it is crucial to carry out the RBFNN-based identification on long data sets and to excite the system within the whole range of operation.

In the following, the proposed linearized control model will be used for standard MPC.

B. Numerical results with EPANET

Taking into account varying electricity prices, operational and physical constraints, the standard MPC scheme has been tested. The results obtained using the EPANET model simulating the real environment are presented below.

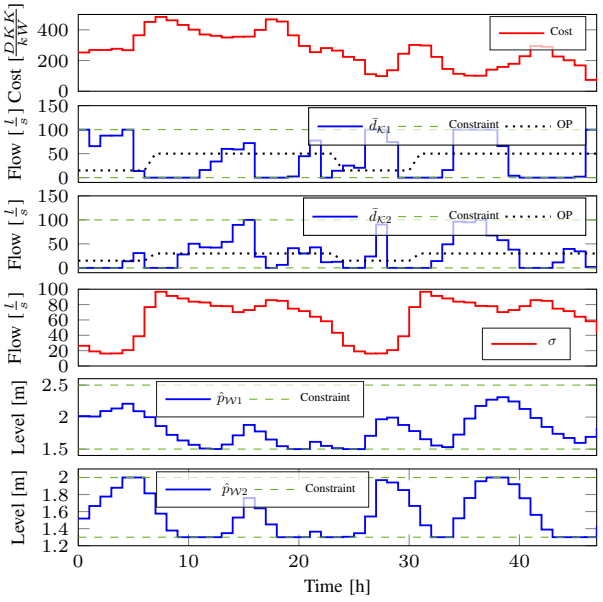

Fig. 6. Input and state evaluation on the EPANET model under MPC.

In Fig 6., the control signals at the peak electricity are decreasing and the actuation is shifted towards the less expensive period in the night. Here, a prediction horizon $H_p = 24$ has been used. From the level signal it is evident that the reservoir is filled when the energy price is low and empties when the energy price is high. Note that the level variation in $\mathcal{W}1$ is one meter and 0.7 meter in $\mathcal{W}2$.

C. Experimental results

The proposed modelling and control method has also been implemented on a test setup at Aalborg University. This setup represents a $1 : 20$ scaled version of a real WDN. The schematic and physical setup is shown Fig. 7.

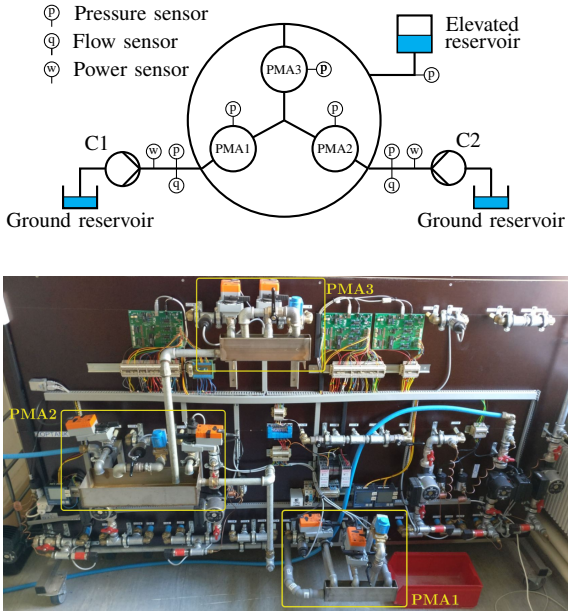

Fig. 7. Schematic (above) and photo (below) of the laboratory setup.

There are two inlet pumps $C1$ and $C2$, supplying a water ring formed around three Pressure Management Areas (PMAs), placed at different elevations. To the main ring, one elevated reservoir is connected. The schematic also indicates the sensors available on the setup. The time constant of the system is approximately 52 minutes, which is low compared to a real WDN. Therefore, the consumption and price profiles have been compressed accordingly. The control algorithm has been implemented with $H_p = 2$ hours and the overall test time was four hours, equivalent to two days in real life. Note, that in this specific test scenario the varying cost is a simple sinusoidal which follows the total flow consumption. The measurements showing the results of the implemented control are shown in Fig. 8.

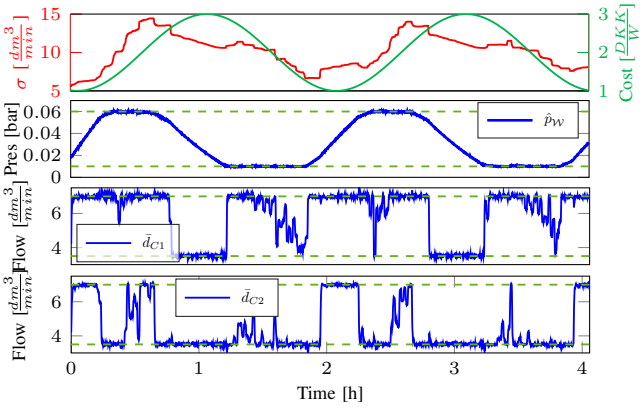

Fig. 8. Measurements: σ consumption, $\hat{p}$ tank pressure and $\bar{d}$ inlet flow.

The sinusoidal cost function is a simplification, representing a possible agreement between utilities and energy providers. This typically means low prices during night and high cost during the daytime. The daily consumption rate σ has been generated by controlling two outlet valves in each PMAs. This valve control rule follows a periodic pattern, mimicking a typical daily flow consumption rate.

The algorithm has been implemented with soft constraints to avoid infeasibility and thereby system failure. The on-line test results above show the feasibility of the proposed control strategy, while guaranteeing appropriate safety objectives. Note that the pumps cannot shut down completely as in real life, due to the lack of non-return valves on the inlets. Therefore, the inflow is kept at a minimum when the tank is being emptied. In addition to the control results, Fig. 9. illustrates pressure measurements in the PMAs.

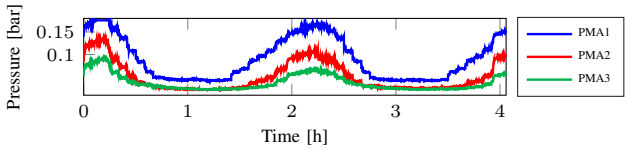

Fig. 9. Pressure in the critical points.

The pressure variation in the PMAs is around 0.1 bar which is considered high. With the proposed constraints, and test setup it has not been possible to reduce this variation, especially not in the PMA where the elevated reservoir is connected. A solution to this is to keep higher pressure in the elevated reservoir and allow less variation in the MPC.

The pump power consumption with the proposed MPC have been compared with on/off control. The sum of the power consumption at the two inlets are shown in Fig. 10.

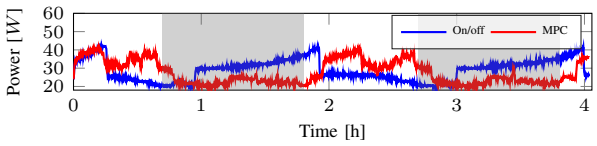

Fig. 10. Comparison of power consumption.

One of the features of on/off control is that typically the storage tanks get emptied at the time when the consumption increases together with the energy prices. The areas marked with grey belong to the cost-expensive period of the day. As Fig. 10 indicates, pumping stations under on/off control must turn on in these expensive periods to fill up the storage tanks again.

For accumulated economic cost comparison, 14 hours long measurements have been carried out which account for a whole week in real-life. The money used on electricity yielded approximately ten percent less than in case of on/off control, see Fig. 11.

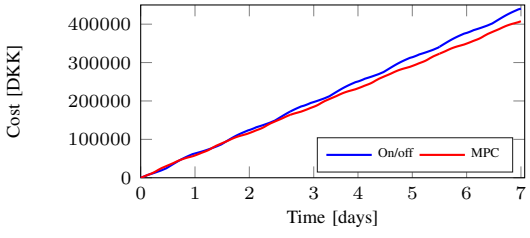

Fig. 11. Accumulated economic cost comparison.

It is reasonable to compare the accumulated cost in the end of each period, as we minimize the economic cost over an H_p = 24 hours long horizon.

VI. CONCLUSIONS

We proposed a reduced model for describing elevated reservoir dynamics and pressures in water distribution networks with multiple inlets. The proposed model structure has been used to identify Neural Network-based models relying on data available at inlet points and in storage tanks. We have shown that if we linearize the NN-model in the two peak points of the total demand, the resulting LTV model represents the network with good prediction accuracy and thereby suitable for the internal model of standard MPC. The proposed model has been tested with standard Model Predictive Control. Results on a simulation model of a real distribution network from Denmark, along with experimental tests with a scaled lab setup have demonstrated feasibility and cost savings. The proposed methods are considered Plug&Play in the sense that only data and structural assumptions have been used in our design.

ACKNOWLEDGMENT

The authors would like to thank Peter Nordahn and Verdo A/S for the insightful discussions and for providing data and the EPANET model of the city Randers in Denmark.

REFERENCES

[1] L. A. Rossman, *EPANET 2 Users Manual*. 2008.
[2] Y. Wang, J. R. Salvador, D. M. de la Peña, V. Puig, and G. Cembrano, "Periodic Nonlinear Economic Model Predictive Control with Changing Horizon for Water Distribution Networks," *IFAC Proceedings Volumes*, vol. 50, no. 1, pp. 6588–6593, 2017.
[3] Y. Wang, G. Cembrano, V. Puig, M. Urrea, J. Romera, D. Saporta, J. G. Valero, and J. Quevedo, "Optimal Management of Barcelona Water Distribution Network using Non-linear Model Predictive Control," *IFAC Proceedings Volumes*, vol. 50, no. 1, pp. 5380–5385, 2017.
[4] S. Leirens, C. Zamora, R. Negenborn, and B. D. Schutter, "Coordination in urban water supply networks using distributed model predictive control," in *Proceedings of the 2010 American Control Conference*, (Baltimore, Maryland), pp. 3957–3962, 2010.
[5] C. Ocampo-Martinez, V. Puig, and S. Bovo, "Decentralised MPC based on a graph partitioning approach applied to the Barcelona drinking water network," *IFAC Proceedings Volumes*, vol. 44, no. 1, pp. 1577–1583, 2011.
[6] C. Sun, M. Morley, D. Savic, V. Puig, G. Cembrano, and Z. Zhang, "Combining Model Predictive Control with Constraint-Satisfaction formulation for the operative pumping control in water networks," *Procedia Engineering*, vol. 119, pp. 963–972, 2015.
[7] C. S. Kallesoe, T. N. Jensen, and R. Wisniewski, "Adaptive reference control for pressure management in water networks," in *European Control Conference (ECC)*, (Linz), pp. 3268–3273, 2015.
[8] T. N. Jensen, C. S. Kallesøe, J. D. Bendtsen, and R. Wisniewski, "Plug-and-play Commissionable Models for Water Networks with Multiple Inlets," in *European Control Conference (ECC)*, (Limassol), pp. 2971–2976, 2018.
[9] C. S. Kallesøe, T. N. Jensen, and J. D. Bendtsen, "Plug-and-Play Model Predictive Control for Water Supply Networks with Storage," *IFAC Proceedings Volumes*, vol. 50, no. 1, pp. 6582–6587, 2017.
[10] P. K. Swamee and A. K. Sharma, *Design of Water Supply Pipe Networks*. John Wiley & Sons, Inc., 2013.
[11] N. Deo, *Graph Theory with Applications to Engineering and Computer Science*. Prentice-Hall, 1st ed., 1974.
[12] J. Liu, *Radial basis function (RBF) neural network control for mechanical systems: Design, analysis and matlab simulation*. Beijing: Springer, 2013.
[13] H. Madsen, *Time Series Analysis*. Chapman & Hall, 2nd ed., 2008.
[14] K. M. H. Baunsgaard, O. Ravn, C. S. Kallesøe, and N. K. Poulsen, "MPC control of water supply networks," in *European Control Conference (ECC)*, pp. 1770–1775, 2016.
[15] C. Kallesøe, J. Aarestrup, and K. Rokkjær, "Energy optimization for booster sets," *World Pumps*, vol. 1, no. 12, pp. 24, 26–30, 2011.